Supplemental Information

Multi-species activity screening of microcin J25 mutants yields antimicrobials with increased specificity towards pathogenic *Salmonella* species relative to human commensal *Escherichia coli*

Seth C. Ritter, Mike L. Yang, Yiannis N. Kaznessis, Benjamin J. Hackel

Department of Chemical Engineering and Materials Science, University of Minnesota–Twin Cities, Minneapolis, Minnesota

Supplemental Data and Analysis

Algorithm to measure zones of inhibition

Sizes of zones of inhibition were measured using a custom MATLAB script (see attached code and example). This script works according to the following pseudocode:

1. Import image, downscale and apply a median smoothing to reduce noise
2. User selects starting pixel within the colony of the producing bacteria
3. Algorithm steps out to adjacent pixels, adding them to the set of colony pixels if their intensity is above some fraction (user defined, default to 0.95) of the average of added colony pixels.
4. Pixels which are surrounded by colony pixels are automatically added to the colony pixels and assumed to be image errors or inconsistency in growth region.
5. Algorithm then steps out from boundary of colony pixels to add zone of inhibition pixels, adding pixels below some user fraction of the average (default to 1.0).
6. Surrounded pixels are added as well
7. Program outputs the size of each zone in pixels

Below is an example output:

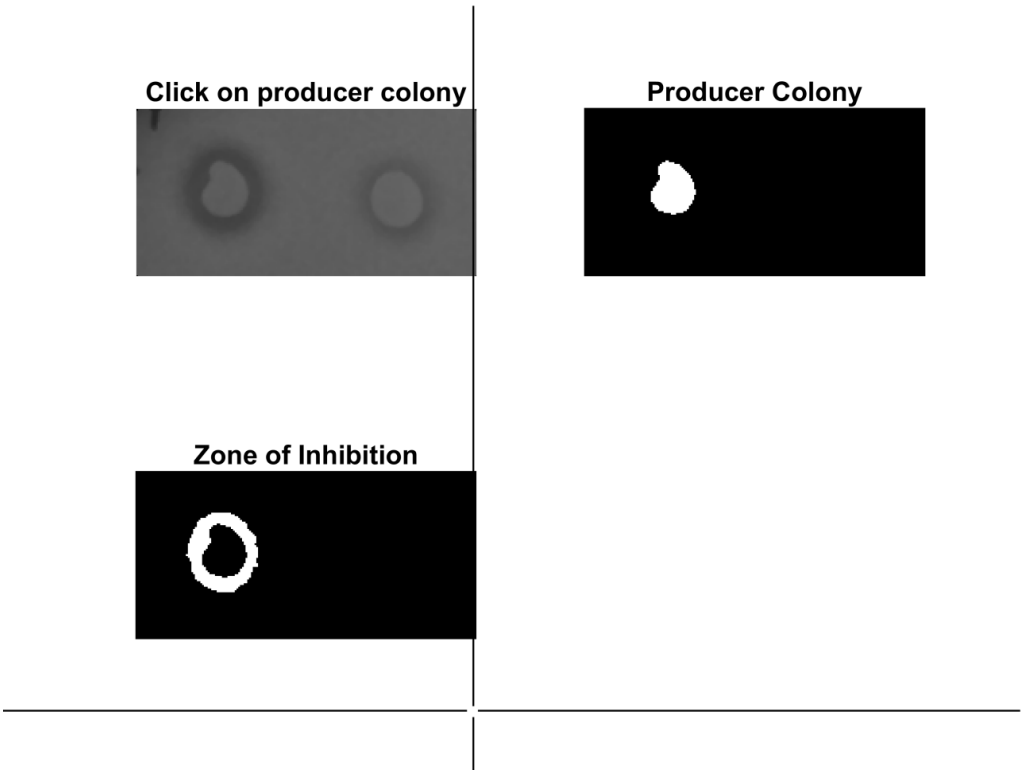

Supplemental Figure 1. Automated measuring of zones of inhibition

(Top-left) Imported and smoothed image taken by user showing two producer colonies surrounded by zones of inhibition as a result of antimicrobial production. (Top-right) Upon selection of the left producer colony, the algorithm generates the displayed producer colony (size = 531 pixels). (Bottom-left) The algorithm displays the zone of inhibition (size = 807 pixels).

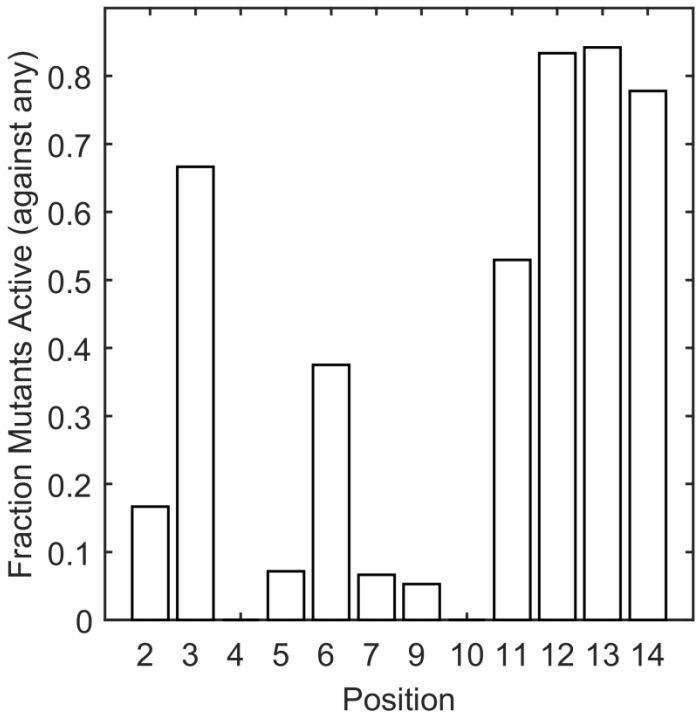

Supplemental Figure 2. Per-residue mutational tolerance.

Displayed are the fractions of sampled mutants (n = 14-18 per site) which retained detectable activity against any of the four targets are presented. The analysis finds that loop positions 11-14 form the continuous set of residues with the highest mutational tolerance. Positions 7 and 9 are known to have a low tolerance for mutation. Pavlova et al showed that mutating positions 7 and 9 reduced RNAP inhibition.

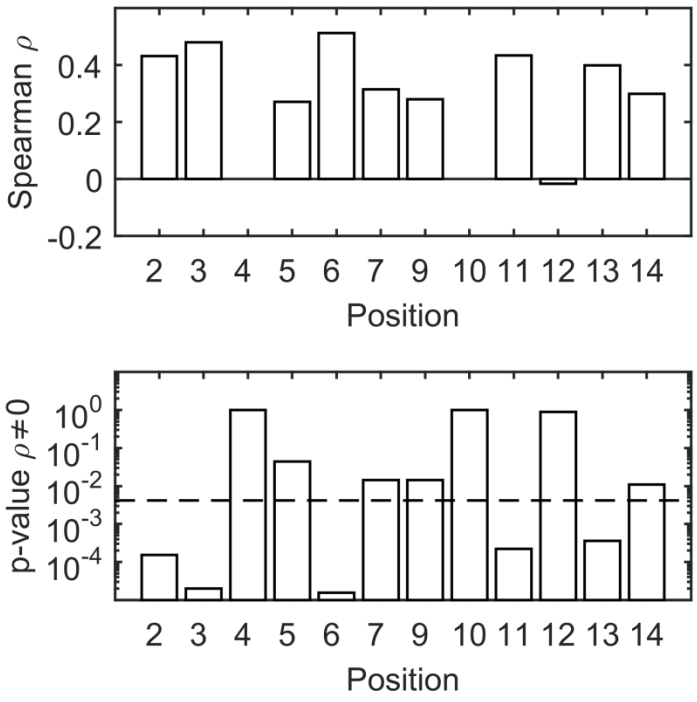

Supplemental Figure 3. Relationship between chemical homology and MccJ25 mutant activity per residue.

Chemical homology, a global relationship of the tendencies of different amino acid substitutions at evolutionarily related sites, was assessed as a predictor of activity of MccJ25 single-mutants. For each position the correlation between activities, against all four pathogenic targets of mutants sampled, and the BLOSUM 90 score associated with the (wild-type, mutant) pair was analyzed.

It is found that 5 of 12 positions tested show a significant Spearman's correlation ($p<0.05$, Bonferri corrected, dashed line bottom plot. Computed using exact permutation.). Position 2 shows a preference for small amino acids, G2[A,C,S]. Position 3 shows a preference for small amino acids, A3[G,C,S,T], but also supports many others. However, many mutations show differences between the different targets, implying that this interaction may serve to enable some specificity. Though position 5 showed conservation amongst mutations sampled, as well as supporting literature data (Lai and Kaznessis, 2017) (requiring charged residue), only 1 other mutation was tolerated and sampled (H5R), which was insufficient evidence for testing. Position 6 shows a preference for hydrophobic residues, V6[L,I,W,F].

Position 11 shows a preference for hydrophobic residues, V11[I,M,W]. Position 13 shows a small preference for hydrophobic residues, I13[F,W,Y,M,L,V,A], but also tolerates many hydrophilic mutations. Surprisingly, though positions 12 and 14 show a high tolerance for mutation, they don't show a relationship between the BLOSUM90 scores for mutants in reference to wild-type (Glycine). These data could be explained by the lack of a meaningful interaction between residues 12 and 14 of MccJ25 and any proteins in the host involved in transport or activity.

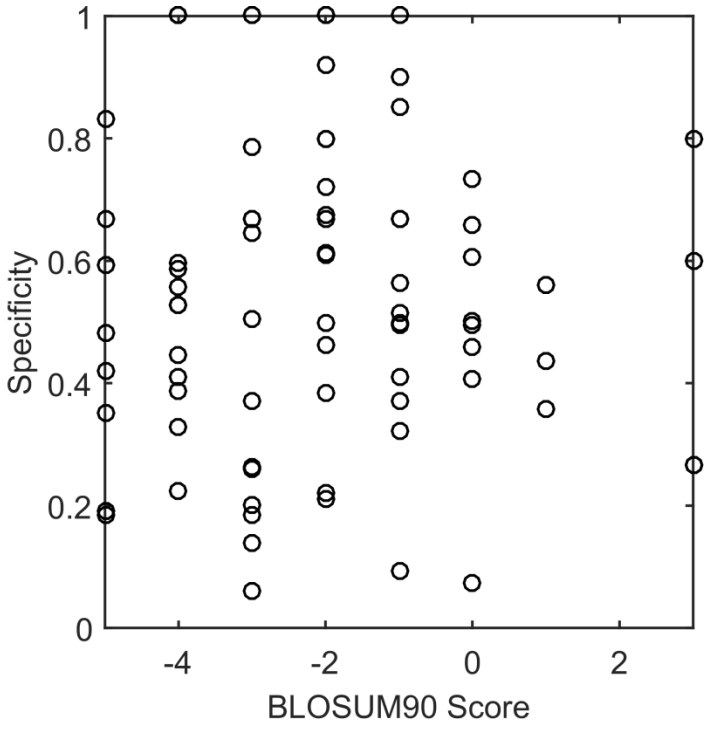

Supplemental Figure 4. Correlation between specificity and chemical homology

Similar to the analysis done in Supplemental Figure 2, the relationship between chemical homology and specificity for each single-mutant was assessed. There is insufficient evidence that chemical homology between wild type and mutant predict the specificity ($p > 0.1$).

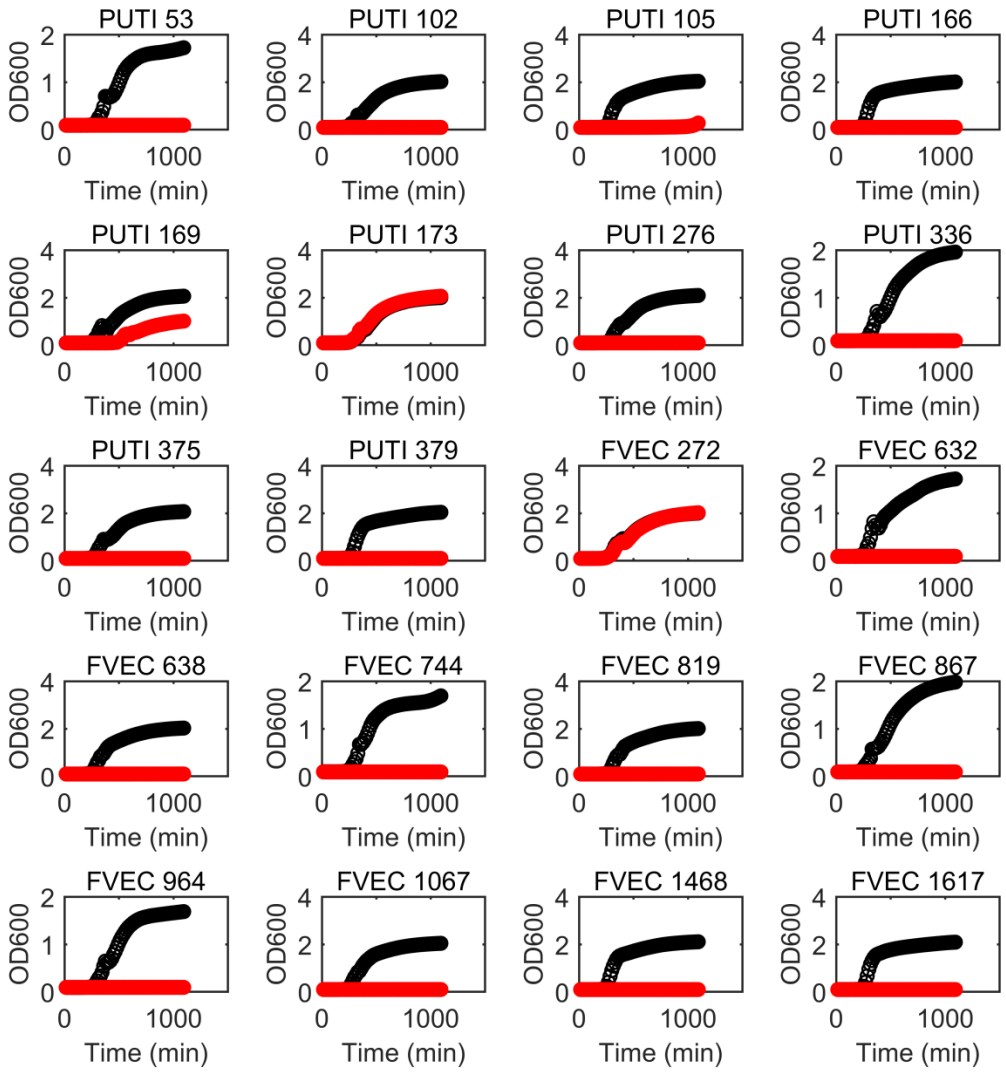

Supplemental Figure 5. Evaluation of commensal E. coli susceptibility to wild-type MccJ25

Commensal *E. coli* isolates were grown overnight to stationary phase in LB. The following day they were diluted 1000x in fresh LB supplemented to 20 vol% sterilized supernatant from a MccJ25 -producing cell line. Their growth was then monitored at 37°C via optical density readings to observe the impact of MccJ25 -containing supernatant on growth. Of the 20 isolates evaluated, 18 showed susceptibility to MccJ25 . The above are averages of 2 replicates per isolate exposed to both MccJ25 (red) and stop-codon mutated MccJ25 (black) supernatant. PUTI 173 and FVEC 272 do not show susceptibility to MccJ25.

A

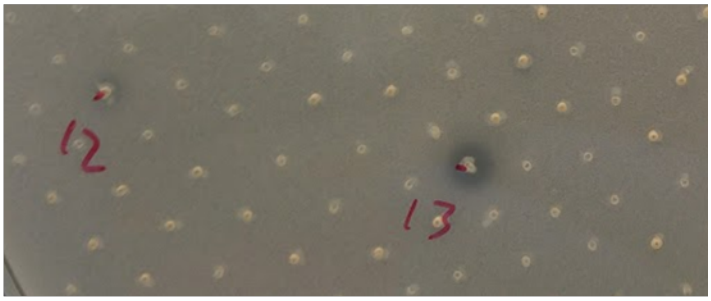

B

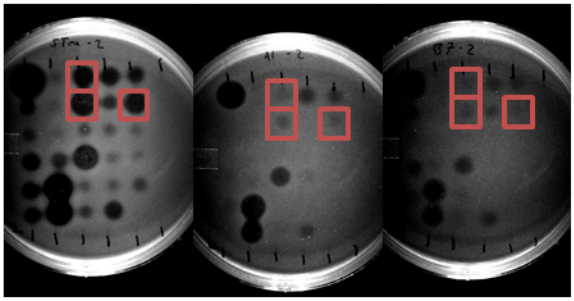

C

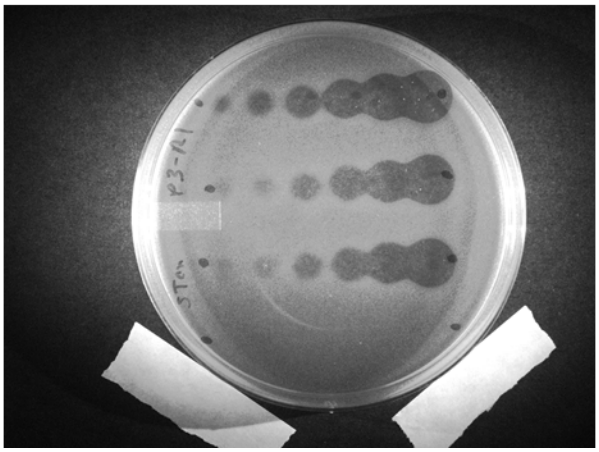

Supplemental Figure 6. Screening strategy for multi-mutant MccJ25 library

(A) Colonies of randomly-selected producers of mutants of MccJ25 were transferred to LB-agar plates seeded with SE and IPTG. Following outgrowth, colonies showing zones of inhibition were gathered. (B) Heat-sterilized supernatants produced from the 64 active colonies from (A) were assayed for activity

against pathogenic strains as well as human commensal *E. coli*. In the examples displayed, the orange boxes outline clones that were sequence-verified to be MccJ25^{I13T}. The differential response in acitivity between STen (left) and two human commensal *E. coli* strains (middle, right) can be seen. (C) Activities of supernatants of candidate producers showing promising specificity modulation in (B) were quantified via dilution-series against all pathogens and human commensal *E. coli*.

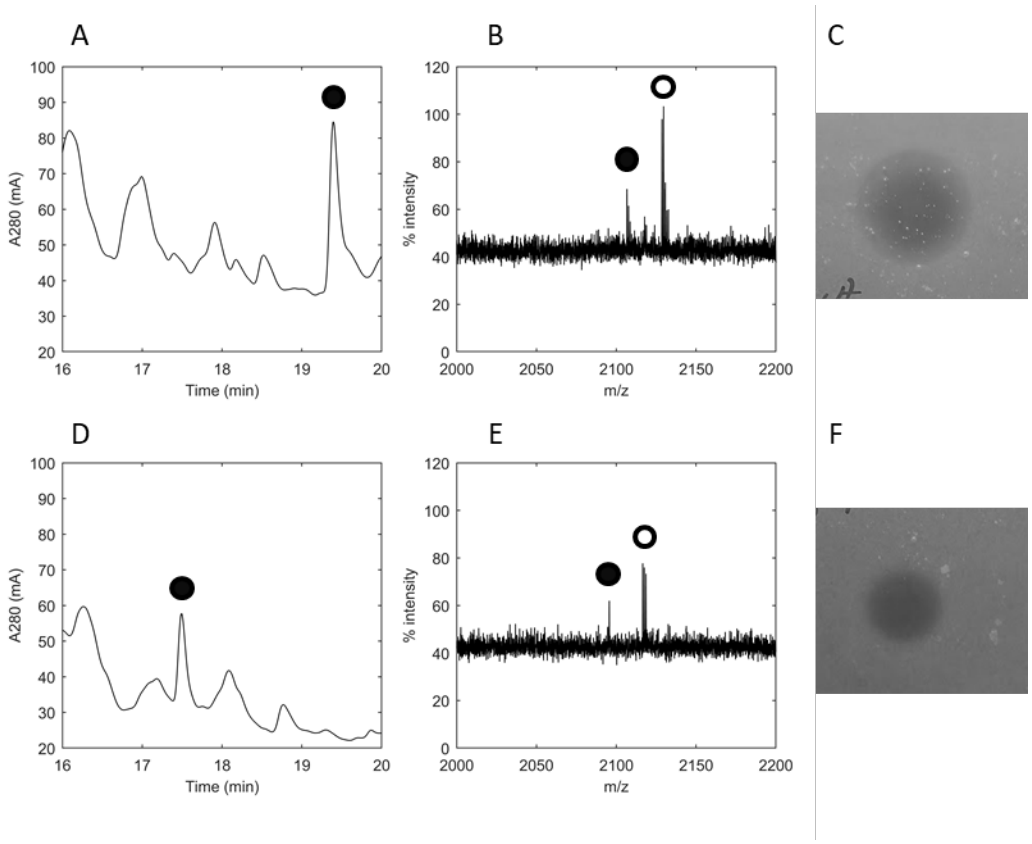

Supplemental Figure 7. Assessment of activity of purified MccJ25 and MccJ25^{I13T}

MccJ25 (A-C) and MccJ25^{I13T} (D-F) were purified from supernatant of expressing cells. Following a 2-volume n-butanol extraction, samples were dried and run on RP-HPLC (A, D). All peaks absorbing at 280 nm were collected and evaluated for activity. Only the indicated peaks (closed circles) displayed activity against the *Salmonella* indicator strain. To assess identity, active peaks were freeze-dried under vacuum, resuspended in ultrapure water and evaluated via matrix-assisted laser-desorption ionization mass spectrometry (B, E). The processed form (closed circle) and linear form (open circle) of MccJ25 and MccJ25^{I13T} were identified. Previous efforts in the literature have demonstrated that the linear form is not active (Wilson et al., 2003). Water-solubilized purified peptides exhibited activity against *Salmonella* indicator strain in an agar plate assay analogous to Figure 4 (C, F).

Supplemental Table I. Bacteria and plasmids used

Bacterial Strain or Plasmid	Description	Reference or Source
Producer		
NEB Express I^{q}	BL21 derivative, no antimicrobial peptides, overexpresses LacI	New England Biolabs
Pathogenic Targets		
***Salmonella enterica* serovar Enteritidis**	#MH9189	Timothy Johnson, Veterinary and Biological Science, University of Minnesota
***Salmonella enterica* serovar Tennessee**	#ST101	Timothy Johnson, Veterinary and Biological Science, University of Minnesota
***Escherichia coli* JJ1887**	Urinary tract infection causing	J. Johnson, Veterans Affairs Hospital, Minneapolis, MN
***Escherichia coli* O157:H7**	#2026	Michael Sadowsky, Biotechnology Institute, University of Minnesota
Commensal Targets		
***Escherichia coli* PUTI 53**	Human isolate. Sourced sample type: Urine	J. Johnson, Veterans Affairs Hospital, Minneapolis, MN
***Escherichia coli* PUTI 102**	Human isolate. Sourced sample type: Urine	J. Johnson, Veterans Affairs Hospital, Minneapolis, MN
***Escherichia coli* PUTI 105**	Human isolate. Sourced sample type: Urine	J. Johnson, Veterans Affairs Hospital, Minneapolis, MN
***Escherichia coli* PUTI 166**	Human isolate. Sourced sample type: Urine	J. Johnson, Veterans Affairs Hospital, Minneapolis, MN
***Escherichia coli* PUTI 169**	Human isolate. Sourced sample type: Urine	J. Johnson, Veterans Affairs Hospital, Minneapolis, MN
***Escherichia coli* PUTI 173**	Human isolate. Sourced sample type: Urine	J. Johnson, Veterans Affairs Hospital, Minneapolis, MN
***Escherichia coli* PUTI 276**	Human isolate. Sourced sample type: Urine	J. Johnson, Veterans Affairs Hospital, Minneapolis, MN
***Escherichia coli* PUTI 336**	Human isolate. Sourced sample type: Fecal	J. Johnson, Veterans Affairs Hospital, Minneapolis, MN
***Escherichia coli* PUTI 375**	Human isolate. Sourced sample type: Fecal	J. Johnson, Veterans Affairs Hospital, Minneapolis, MN
***Escherichia coli* PUTI 379**	Human isolate. Sourced sample type: Fecal	J. Johnson, Veterans Affairs Hospital, Minneapolis, MN
***Escherichia coli* FVEC 272**	Human isolate. Sourced sample type: Fecal	J. Johnson, Veterans Affairs Hospital, Minneapolis, MN
***Escherichia coli* FVEC 632**	Human isolate. Sourced sample type: Fecal	J. Johnson, Veterans Affairs Hospital, Minneapolis, MN
***Escherichia coli* FVEC 638**	Human isolate. Sourced sample type: Fecal	J. Johnson, Veterans Affairs Hospital, Minneapolis, MN
***Escherichia coli* FVEC 744**	Human isolate. Sourced sample type: Fecal	J. Johnson, Veterans Affairs Hospital, Minneapolis, MN
***Escherichia coli* FVEC 819**	Human isolate. Sourced sample type: Fecal	J. Johnson, Veterans Affairs Hospital, Minneapolis, MN
***Escherichia coli* FVEC 867**	Human isolate. Sourced sample type: Fecal	J. Johnson, Veterans Affairs Hospital, Minneapolis, MN
***Escherichia coli* FVEC 964**	Human isolate. Sourced sample type: Fecal	J. Johnson, Veterans Affairs Hospital, Minneapolis, MN
***Escherichia coli* FVEC 1067**	Human isolate. Sourced sample type: Fecal	J. Johnson, Veterans Affairs Hospital, Minneapolis, MN
***Escherichia coli* FVEC 1468**	Human isolate. Sourced sample type: Fecal	J. Johnson, Veterans Affairs Hospital, Minneapolis, MN
***Escherichia coli* FVEC 1617**	Human isolate. Sourced sample type: Fecal	J. Johnson, Veterans Affairs Hospital, Minneapolis, MN
Plasmid		
pJP3	Microcin J25 expression cassette containing plamid. McjA under Laco/T5 for controlled induction.	Link group, Princeton (Pan et al., 2010)
pJP4	pJP3 variant with XhoI moved downstream and optimized ribosomal binding site	This work

Supplemental Table II. Sequences for genes and oligonucleotides used

pJP4	
Modified mcjA expression cassette	CCCTTTCGTCTTCACCTCGATCGATCATAAAAAATTTATTTGCTTTGTGAGCGGATAACAATTATAATACTCGAGGCGCC AGTCTCCCCATAAGGAGGTTAACATACATGATCAAACATTTTCACTTCAACAAACTGTCAAGCGGTAAGAAGAATAATGT TCCGAGCCCAGCAAAGGGAGTGATTCAGATTAAGAAGAGCGCCTCGCAATTAACGAAGGGCGGTGCTGGTCATGTCCCTG AATATTTCGTGGGCATCGGGACCCCAATCTCCTTCTATGGGTAAAAGCTTAATTAGCTGAGCTTGGACTC
Single-site saturation mutagenesis	
mcjaFWD1	AATTCTCGAGGCGCCAGTCTCCCCATAAGGAGGTTAACATACATGATCAAACATTTTCAC
mcjaFWD2	TACATGATCAAACATTTTCACTTCAACAAACTGTCAAGCGGTAAGAAGAATAATGTTCCG
mcjaFWD3	GTAAGAAGAATAATGTTCCGAGCCCAGCAAAGGGAGTGATTCAGATTAAGAAGAGCGCCT
mcjaFWD4	TCAGATTAAGAAGAGCGCCTCGCAATTAACGAAG
mcjaFWD4_lib_3'_set1	GAATATTTCGTGGGCATCGGGACCCCAATCTCCTTCTATGGGTAAAAGCTTAGCCGACCG
mcjaFWD4_lib_5'_set2	GCGCCTCGCAATTAACGAAGGGCGGTGCTGGTCATGTCCC
mcjaFWD4_lib_3'_set2	ACCCCAATCTCCTTCTATGGGTAAAAGCTTAGCCGACCG
mcjaFWD4_lib_5'_set3	GGCGGTGCTGGTCATGTCCCTGAATATTTCGTGGGCATCG
mcjaFWD_lib_5'_lib2	GCGCCTCGCAATTAACGAAGGGCNNKGCTGGTCATGTCCCTGAATATTTCGTGGGCATCG
mcjaFWD_lib_5'_lib3	GCGCCTCGCAATTAACGAAGGGCGGTNNKGGTCATGTCCCTGAATATTTCGTGGGCATCG
mcjaFWD_lib_5'_lib4	GCGCCTCGCAATTAACGAAGGGCGGTGCTNNKCATGTCCCTGAATATTTCGTGGGCATCG
mcjaFWD_lib_5'_lib5	GCGCCTCGCAATTAACGAAGGGCGGTGCTGGTNNKGTCCCTGAATATTTCGTGGGCATCG
mcjaFWD_lib_5'_lib6	GCGCCTCGCAATTAACGAAGGGCGGTGCTGGTCATNNKCCTGAATATTTCGTGGGCATCG
mcjaFWD_lib_5'_lib7	GCGCCTCGCAATTAACGAAGGGCGGTGCTGGTCATGTCNNKGAATATTTCGTGGGCATCG
mcjaFWD_lib_5'_lib9	GGCGGTGCTGGTCATGTCCCTGAANNKTTCGTGGGCATCGGGACCCCAATCTCCTTCTAT
mcjaFWD_lib_5'_lib10	GGCGGTGCTGGTCATGTCCCTGAATATNNKGTGGGCATCGGGACCCCAATCTCCTTCTAT
mcjaFWD_lib_5'_lib11	GGCGGTGCTGGTCATGTCCCTGAATATTTCNNKGGCATCGGGACCCCAATCTCCTTCTAT
mcjaFWD_lib_5'_lib12	GGCGGTGCTGGTCATGTCCCTGAATATTTCGTGNNKATCGGGACCCCAATCTCCTTCTAT
mcjaFWD_lib_5'_lib13	GGCGGTGCTGGTCATGTCCCTGAATATTTCGTGGGCNNKGGGACCCCAATCTCCTTCTAT
mcjaFWD_lib_5'_lib14	GGCGGTGCTGGTCATGTCCCTGAATATTTCGTGGGCATCNNKACCCCAATCTCCTTCTAT
REV_amplify_10_03_16	CGGTCGGCTAAGCTTTTA
Multi-site saturation mutagenesis	
Lib3s1_Lib13s1	CCTCGCAATTAACGAAGGGCRSCRMCGGACACBTCCCAGAATACTTCRTGGGATMCGSAACCCCAATCTCCTTCTATGG
Lib3s2_Lib13s1	CCTCGCAATTAACGAAGGGCRSCATGGGACACBTCCCAGAATACTTCRTGGGATMCGSAACCCCAATCTCCTTCTATGG
Lib3s1_Lib13s2	CCTCGCAATTAACGAAGGGCRSCRMCGGACACBTCCCAGAATACTTCRTGGGAAYAGSAACCCCAATCTCCTTCTATGG
Lib3s2_Lib13s2	CCTCGCAATTAACGAAGGGCRSCATGGGACACBTCCCAGAATACTTCRTGGGAAYAGSAACCCCAATCTCCTTCTATGG
FWD1	TATAATACTCGAGGCGCCAGTCTCCCCATAAGGAGGTTAACATACATGATCAAACATTTT
FWD2	ACATACATGATCAAACATTTTCACTTCAACAAACTGTCAAGCGGTAAGAAGAATAATGTT
FWD3	GCGGTAAGAAGAATAATGTTCCGAGCCCAGCAAAGGGAGTGATTCAGATTAAGAAGAGCG
FWD4	GATTCAGATTAAGAAGAGCGCCTCGCAATTAACGAAGGGC
REV	AGCTAATTAAGCTTTTACCCATAGAAGGAGATTGGGGT
Next-generation Sequencing	
TSUA1	AATGATACGGCGACCACCGAGATCTACACTCTTTCCCTACACGACGCTCTTCCGATCT
BarcodeR1	ACACGACGCTCTTCCGATCTCTAGGCGCCTCGCAATTAACGAAG
BarcodeR2	ACACGACGCTCTTCCGATCTCATAGCGCCTCGCAATTAACGAAG
BarcodeR3	ACACGACGCTCTTCCGATCTATATGCGCCTCGCAATTAACGAAG
BarcodeR4	ACACGACGCTCTTCCGATCTTCTAGCGCCTCGCAATTAACGAAG
BarcodeR5	ACACGACGCTCTTCCGATCTTACGGCGCCTCGCAATTAACGAAG
BarcodeR6	ACACGACGCTCTTCCGATCTGCGTGCGCCTCGCAATTAACGAAG
BarcodeR7	ACACGACGCTCTTCCGATCTTGGCGCGCCTCGCAATTAACGAAG
BarcodeR8	ACACGACGCTCTTCCGATCTGACTGCGCCTCGCAATTAACGAAG
BarcodeC1	AGACGTGTGCTCTTCCGATCACCGCTCAGCTAATTAAGCTTTTA
BarcodeC2	AGACGTGTGCTCTTCCGATCTGGTCTCAGCTAATTAAGCTTTTA
BarcodeC3	AGACGTGTGCTCTTCCGATCTCTACTCAGCTAATTAAGCTTTTA
BarcodeC4	AGACGTGTGCTCTTCCGATCCAGTCTCAGCTAATTAAGCTTTTA
BarcodeC5	AGACGTGTGCTCTTCCGATCCTACCTCAGCTAATTAAGCTTTTA
BarcodeC6	AGACGTGTGCTCTTCCGATCGGCACTCAGCTAATTAAGCTTTTA
BarcodeC7	AGACGTGTGCTCTTCCGATCAGTGCTCAGCTAATTAAGCTTTTA
BarcodeC8	AGACGTGTGCTCTTCCGATCCAACCTCAGCTAATTAAGCTTTTA
BarcodeC9	AGACGTGTGCTCTTCCGATCCTGCCTCAGCTAATTAAGCTTTTA
BarcodeC10	AGACGTGTGCTCTTCCGATCGAGTCTCAGCTAATTAAGCTTTTA
BarcodeC11	AGACGTGTGCTCTTCCGATCCGTGCTCAGCTAATTAAGCTTTTA
BarcodeC12	AGACGTGTGCTCTTCCGATCTTAACTCAGCTAATTAAGCTTTTA
TSI3'	CAAGCAGAAGACGGCATACGAGATCGTGATGTGACTGGAGTTCAGACGTGTGCTCTTCCG

Supplemental Table III. Codon usage and multi-mutant library activity

		Codon		Codon Usage (Nakamura et al., 1999)[a]		Activity vs SE	
Position	Amino Acid	Singletons	Multi-mutant	Singletons	Multi-mutant	Singletons	Multi-mutant
2	T	ACG	ACC	8.5	14.3	0	1
2	S	TCT	AGC	21.2	15.9	0.8	0
2	A	GCG	GCC	54.9	14.1	0.6	1
2	G	GGT	GGC	14.3	14.3	1	1
3	M	ATG	ATG	8.5	8	0.6	1
3	N	AAT	AAC	32.6	19.6	0.5	0
3	T	ACG	ACC	14.6	25.2	0.7	1
3	D	GAT	GAC	32.6	25.5	0	1
3	A	GCT	GCC	24.4	33.1	1	1
6	L	CTG	CTC	37.4	37.4	0.3	0
6	V	GTC	GTC	14.6	25.2	1	0
6	F	TTT	TTC	30	15.1	0.5	1
11	M	ATG	ATG	13.8	25.5	0.4	1
11	V	GTG	GTG	28.9	18.8	1	1
13	Y	TAT	TAC	37.4	37.4	0.5	1
13	S	TCT	TCC	33.9	33.9	0.5	0
13	T	ACG	ACA	18.6	8.5	0.5	1
13	I	ATC	ATC	14.6	6.1	1	1
14	A	GCG	GCA	37.4	37.4	0.7	0
14	G	GGG	GGA	14.3	8.2	1	1

[a]Codon usage estimated for *Escherichia coli*

It is found that only 50% of inactive singletons from the multi-mutants library can be explained by codon usage differences. The p-values for the grid of comparisons do not support codon usage predicting activities of singletons in the multi-mutant library ($p > 0.1$).

Supplemental References

Lai PK, Kaznessis YN. 2017. Free Energy Calculations of Microcin J25 Variants Binding to the FhuA Receptor. *J. Chem. Theory Comput.* **13**:3413–3423.

Nakamura Y, Gojobori T, Ikemura T. 1999. Codon usage tabulated from the international DNA sequence databases; its status 1999. *Nucleic Acids Res.* **27**:292.

Pan SJ, Cheung WL, Link AJ. 2010. Engineered gene clusters for the production of the antimicrobial peptide microcin J25. *Protein Expr. Purif.* **71**:200–206.

Wilson K-A, Kalkum M, Ottesen J, Yuzenkova J, Chait BT, Landick R, Muir T, Severinov K, Darst SA. 2003. Structure of microcin J25, a peptide inhibitor of bacterial RNA polymerase, is a lassoed tail. *J. Am. Chem. Soc.* **125**:12475–12483.